Human Molecular Genetics, 2013, Vol. 22, No. 2 **300–312**
doi:10.1093/hmg/dds429
Advance Access published on October 16, 2012

22q11 Gene dosage establishes an adaptive range for sonic hedgehog and retinoic acid signaling during early development

Thomas M. Maynard[1,†], Deepak Gopalakrishna[2,†], Daniel W. Meechan[1], Elizabeth M. Paronett[1], Jason M. Newbern[3] and Anthony-Samuel LaMantia[1,*]

[1]GW Institute for Neuroscience and Department of Pharmacology and Physiology, The George Washington University School of Medicine and Health Sciences, Washington DC, USA [2]Curriculum in Genetics and Molecular Biology, University of North Carolina, Chapel Hill, NC, USA and [3]Neuroscience Center, University of North Carolina School of Medicine, Chapel Hill, NC 27599, USA

Received July 3, 2012; Revised September 4, 2012; Accepted October 8, 2012

We asked whether key morphogenetic signaling pathways interact with 22q11 gene dosage to modulate the severity of cranial or cardiac anomalies in DiGeorge/22q1 deletion syndrome (22q11DS). Sonic hedgehog (*Shh*) and retinoic acid (RA) signaling is altered in the brain and heart—clinically significant 22q11DS phenotypic sites—in *LgDel* mouse embryos, an established 22q11DS model. *LgDel* embryos treated with cyclopamine, an *Shh* inhibitor, or carrying mutations in *Gli3*^{Xtj}, an Shh-signaling effector, have morphogenetic anomalies that are either not seen, or seen at significantly lower frequencies in control or single-mutant embryos. Similarly, RA exposure or genetic loss of RA function via heterozygous mutation of the RA synthetic enzyme *Raldh2* induces novel cranial anomalies and enhances cardiovascular phenotypes in *LgDel* but not other genotypes. These changes are not seen in heterozygous *Tbx1* mutant embryos—a 22q11 gene thought to explain much of 22q11DS pathogenesis—in which *Shh* or RA signaling has been similarly modified. Our results suggest that full dosage of 22q11 genes beyond *Tbx1* establish an adaptive range for morphogenetic signaling via Shh and RA. When this adaptive range is constricted by diminished dosage of 22q11 genes, embryos are sensitized to otherwise benign changes in Shh and RA signaling. Such sensitization, in the face of environmental or genetic factors that modify Shh or RA signaling, may explain variability in 22q11DS morphogenetic phenotypes.

INTRODUCTION

DiGeorge or 22q11 deletion syndrome (22q11DS) is the consequence of a hemizygous loss of a 'critical' (1.5 Mb) or larger 'typical' (3 Mb) region of human Chr.22 (1). Clinically significant 22q11DS phenotypes vary in penetrance and severity. They include modest to life-threatening cardiovascular malformations (2,3), mild-to-severe craniofacial and limb anomalies (2), parathyroid and thymic hypoplasia (4) and increased susceptibility to a range of behavioral and psychiatric disorders from autism and intellectual disability to schizophrenia (5). Despite compelling clinical data on varying frequency and severity of 22q11DS phenotypes, there is little mechanistic insight into why shared genomic lesions result in variable outcomes (6,7). Accordingly, we asked whether key morphogenetic signaling pathways, whose activity and influence may vary at 22q11DS phenotypic sites, interact with diminished 22q11 gene dosage to modulate the severity of cranial or cardiac anomalies.

Initial differentiation at all 22q11DS phenotypic sites, including the brain and heart, depends upon morphogenetic interactions between mesenchymal and epithelial tissues mediated by diffusible signals including sonic hedgehog (Shh), retinoic acid (RA), fibroblast growth factors (Fgfs)

*To whom correspondence should be addressed at: Department of Pharmacology and Physiology, Institute for Neuroscience, The George Washington University School of Medicine and Health Sciences, 2300 Eye Street N.W., Washington DC 20037, USA. Email: lamantia@gwu.edu
†These two authors contributed equally to this work.

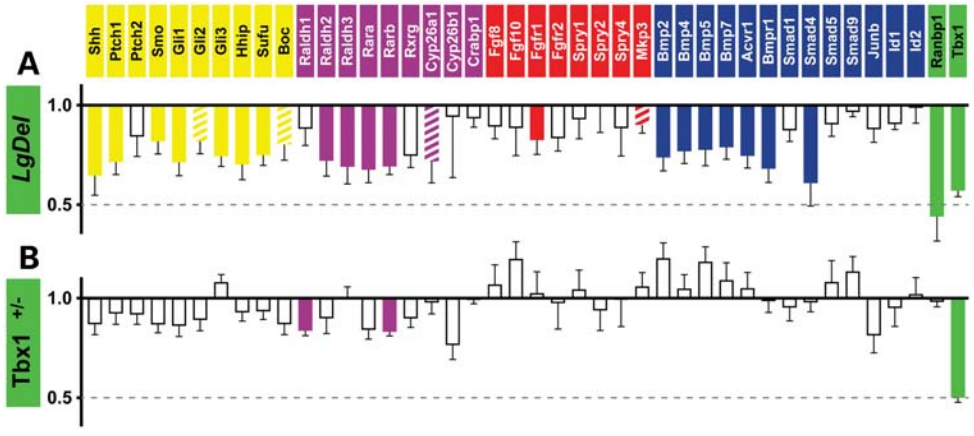

Figure 1. Divergent expression levels of Shh, RA, Fgf and Bmp-related signaling genes assessed by qPCR in whole E10.5 *LgDel* and *Tbx1*$^{+/-}$ and WT littermate control embryos. (**A**) Among 40 candidates, there is significantly diminished expression (relative to WT littermates) of seven Shh-related genes (solid yellow bars; see text for '*n*' and *P*-values), with two additional genes showing a trend toward significant decline (hatched yellow bars). There are RA signaling genes that decline significantly (solid purple bars), plus one additional significant trend (hatched purple bar). One Fgf-related declines significantly (solid red bar), and another shows a significant trend (hatched red bar). Six Bmp-related genes decline significantly (solid blue bars). (**B**) Signaling gene expression in E10.5 *Tbx1*$^{+/-}$ embryos does not mirror *LgDel* changes. There is modest but statistically significant diminished expression of two RA-related genes (solid purple bars), only one of which (*Rarβ*) also declines significantly in the *LgDel*.

and bone morphogenetic proteins (Bmps) (8). Coincident expression of 22q11 genes with these signals in the brain, heart, face and limbs (9–11) suggests that Shh, RA, Fgfs, and Bmps are potential modifiers of 22q11DS phenotypes. Indeed, some phenotypes in mutant mice with genetic disruption of RA (*Raldh2*) and Fgf8 signaling have been identified as 22q11DS 'phenocopies' (12,13), whereas the consequences of Shh and Bmp signaling anomalies are more narrowly interpreted as 'parallel' to 22q11DS (14,15). It is unclear, however, whether such similarities reflect linear effects on common downstream targets consistent with 'phenocopy', or more complex interactions between local signals and 22q11 gene dosage. Shh and RA apparently regulate expression of at least one 22q11 gene, *Tbx1* (16,17). *Tbx1*, when deleted in combination with *Crkl* (outside the critical region, but within the typical region; 1), modulates RA and Fgf8 signaling (18), while total loss of *Tbx1* function down-regulates *Bmp4* (19). Moreover, mutations in RA- as well as Fgf8- and Bmp-associated signaling genes modulate *Tbx1* mutant phenotypes (20–23). *Tbx1* has been robustly associated with several 22q11DS anomalies including aortic arch, thymus and palatal anomalies (24–26). Nevertheless, the role of *Tbx1* in the full 22q11DS spectrum remains uncertain (9,27–29). Thus, we compared the consequences of broader 22q11 deletion versus heterozygous *Tbx1* mutation for altering key morphogenetic signaling pathways and essential 22q11DS phenotypes.

We found that interactions between Shh or RA signaling and 22q11 gene dosage enhance 22q11DS-related phenotypes in the *LgDel* mouse 22q11DS model but not *Tbx1* mutant mice. Alterations of Shh or RA signaling that are otherwise benign yield more frequent and severe cranial or cardiovascular anomalies in *LgDel* mice. Our results do not support simple, linear relationships between morphogenetic signals and 22q11 genes. Instead, 22q11 gene dosage, Shh and RA likely participate in broader homeostatic networks that modulate a dynamic range of signaling for adaptive morphogenesis in the brain, heart and other 22q11DS phenotypic sites. Disruption of these networks by environmental factors or genetic polymorphisms may be an essential contributor to phenotypic variability in 22q11DS.

RESULTS

Diminished 22q11 dosage disrupts inductive signaling pathway gene expression

22q11 gene dosage might influence *Shh*, RA, Fgf or Bmp signaling at 22q11DS phenotypic sites during initial morphogenesis. To assess this potential relationship, we used quantitative PCR to compare expression levels of a subset of *Shh*, *Fgf* or *Bmp* ligands, RA synthetic enzymes, as well as receptors and co-factors for each signal—all with selective expression at 22q11DS phenotypic sites (8)—in *LgDel*, *Tbx1*$^{+/-}$ and wild-type (WT) littermate embryos for each genotype at embryonic day (E) 10.5, a critical stage for morphogenetic interactions.

Nine of 10 representative Shh-signaling genes are diminished by 18–25% in the E10.5 *LgDel* embryo: *Shh* itself, the *Ptc1* co-receptor, *Smo*, an intracellular mediator, *Gli1, Gli2* and *Gli3* transcriptional activator/repressors, and co-factors *Hhip*, *Sufu* and *Boc* ($n = 7$ *LgDel*, 7 WT; 8 genes $P \leq 0.05$; 2 trends, $P \leq 0.06$; Fig. 1). Five of nine representative RA-signaling genes are diminished by 28–32%: synthetic enzymes *Raldh2* and *Raldh3*, RA receptors *Rar*α and *Rar*β and the RA catabolic enzyme *Cyp26a1* ($n = 7$ *LgDel*, 7 WT; 4 genes $P \leq 0.05$; 1 trend $P \leq 0.06$). Two of eight Fgf-related genes decline: the Fgf receptor *Fgfr1* and the Fgf target *Mkp3* (10–18%; $n = 7$ *LgDel*, 7 WT; 1 gene, $P \leq 0.05$; 1 trend $P \leq 0.06$). Finally, six of 13 Bmp-related genes are diminished by 21–39%: four ligands (*Bmp2*, *4*, *5* and *7*), the activin receptor 1 *Acvr1* (a non-selective Tgfβ receptor), the Bmp receptor *Bmpr1* and the non-selective transcriptional mediator *Smad4* ($n = 7$ *LgDel*, 7 WT; 6 genes $P \leq 0.05$).

Tbx1 has been proposed as a key, if not singularly explanatory, 22q11 gene for 22q11DS phenotypes: including aberrant heart and brain development (23,30,31). If *Tbx1* alone is responsible for 22q11DS phenotypes, and if they reflect altered Shh, RA, Bmp or Fgf signaling as suggested (18,32,33), one would expect significant overlap between *Shh*, RA, *Bmp* or *Fgf* signaling gene expression changes in $Tbx1^{+/-}$ and *LgDel* embryos. Of 40 signaling-related genes we assessed, only two are significantly altered in $Tbx1^{+/-}$ versus 22 in *LgDel* embryos ($n = 9$ $Tbx1^{+/-}$; 6 WT; Fig. 1B). Both are RA-signaling genes: *Raldh1* (16% decrease; $P \leq 0.02$; not altered in *LgDel*) and *Rarβ* (17% decrease; $P \leq 0.04$; 31% decrease in *LgDel*). Only *Rarβ* is changed in both $Tbx1^{+/-}$ and *LgDel* embryos; however, the magnitude is significantly greater in *LgDel* embryos ($P \leq 0.04$; $n = 7$ *LgDel*, 9 $Tbx1^{+/-}$). There are no significant expression differences for WT littermates of *LgDel* versus $Tbx1^{+/-}$ embryos of key signaling genes, indicating that expression changes are unlikely due to genetic background effects (Supplementary Material, Fig. S1). The significant changes we identify for both *LgDel* and $Tbx1^{+/-}$ embryos are all decreased expression—including the expected 50% decrement of *Tbx1* itself. We note, however, that we detect increased expression of some of these genes in distinct regions, or in response to pharmacological or genetic manipulation in the LgDel (see in what follows). Apparently, diminished 22q11 gene dosage beyond *Tbx1* distinctly alters morphogenetic signaling gene expression in the *LgDel* model of 22q11DS.

Diminished 22q11 dosage alters *Shh* and RA signaling

The decline in the expression of signaling pathway intermediates does not necessarily mean that signaling via these pathways is altered. Thus, we measured local, independent 'output' of *Shh* and RA signaling—two pathways highly related to 22q11 genes based on previous observations (16–18)—in the head/forebrain and heart in *LgDel* as well as $Tbx1^{+/-}$ embryos. We focused on signaling levels at these sites, and excluded regions like the spinal cord and limb bud where Shh and RA signaling is robust, but 22q11DS phenotypes are less well defined. Thus, we can determine whether there are regional differences in the consequences of diminished 22q11 gene expression for morphogenetic signaling at distinct locations known to be compromised in 22q11DS.

For *Shh*, we crossed a 'knock-in' *Ptch2*:β-galactosidase (βgal) reporter (34) into *LgDel* and $Tbx1^{+/-}$ to visualize and quantify local signaling independent of mRNA levels, which may vary based upon stability. There are neither visible changes in *Ptch2*:βgal patterns nor quantifiable changes in activity (measured by soluble βgal in dissected samples) in the *LgDel* head/forebrain (Fig. 2A and B, top), and there are no changes in *Ptch2*, *Shh* or *Gli1* mRNA levels ($n = 8$ *LgDel*, 9 WT; Fig. 2C, top). In contrast, *Ptch2:*βgal expression expands in the *LgDel* heart/aortic arches (Fig. 2A and B, bottom), and we detect a 25% increase in soluble βgal activity in isolated samples of the cardiac region ($n = 5$ *LgDel*, 5 WT; $P \leq 0.05$, Fig. 2B). We found a parallel increase of *Ptch2* mRNA (45%; $n = 7$ *LgDel*, 9 WT; $P \leq 0.01$), and *Shh* itself is increased by 57% ($n = 7$ *LgDel*, 7 WT; $P \leq 0.019$; Fig. 2C). These changes are not seen in $Tbx1^{+/-}$ embryos for *Ptch2*:βgal activity ($n = 5$ $Tbx1^{+/-}$; 4 WT; Fig. 2D and E) or *Ptch2, Shh* or additional Shh-related signaling genes ($n = 7$ $Tbx1^{+/-}$; 9 WT; Fig. 3F and data not shown).

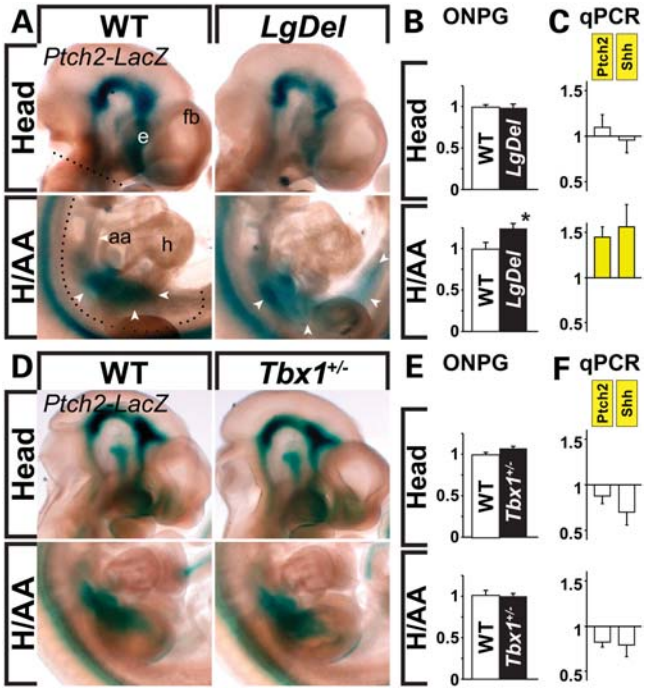

Figure 2. Shh signaling is increased in the developing heart in *LgDel*, but not $Tbx1^{+/-}$ E10.5 embryos. Embryos in (**A**) and (**D**) carry a β-galactosidase (βgal) reporter under the control of the endogenous *Ptch2* promoter. (A) Comparison of *Ptch2*: βgal labeling in the head/forebrain (fb, including the eye, e; top panels; dotted line indicates site of dissection) and heart/aortic arches (H/AA; dotted lines indicated site of dissection) of E10.5 WT (left) and *LgDel* embryos (right). βgal labeling in the nascent heart and aortic arches (arrowheads) is less extensive in WT than *LgDel* embryos (8 *LgDel*, 10 WT embryos analyzed). There is no apparent change in the forebrain/head. Dotted lines in left hand panels indicate regions dissected for quantitative measurements. (**B**) Increased *Ptch2* promoter activation in the heart and aortic arches of the *LgDel* embryos, without change in the head/forebrain, assessed by soluble βgal levels (ONPG assay, see Materials and Methods). (**C**) Increased *Ptch2* and *Shh* mRNA levels in the *LgDel* heart and aortic arches (H/AA; solid yellow bars; *LgDel* values plotted as fold change from WT values = 1), but not in the head/forebrain. (D) No visible difference in cranial or cardiac βgal labeling in WT and $Tbx1^{+/-}$ E10.5 embryos. (**E**) Equivalent levels of βgal activity in the head/forebrain and heart/aortic arches of WT and $Tbx1^{+/-}$ embryos. (**F**) No significant change in *Shh* or *Ptch2* expression in either head or heart of $Tbx1^{+/-}$ embryos.

To measure RA signaling, we bred an RA-indicator transgene (DR5-RARE; 35), which is quantitatively sensitive to altered RA levels (Supplementary Material, Fig. S2), into *LgDel* and $Tbx1^{+/-}$ embryos. In *LgDel* embryos, DR5-RARE-dependent RA signaling appears modestly diminished, based upon altered intensity and extent of βgal labeling, in the head/forebrain and heart/aortic arches (Fig. 3A). In parallel, RA signaling levels (soluble βgal activity in dissected samples) decrease modestly but significantly in the head/forebrain (12%; $n = 6$ *LgDel*; 6 WT; $P \leq 0.05$) and heart (15%; $P \leq 0.05$, Fig. 3B). Expression levels of RA synthetic

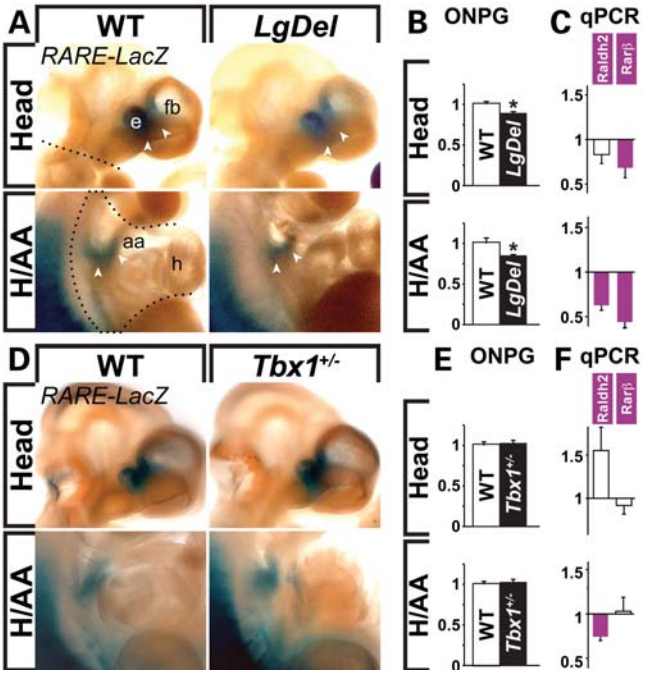

Figure 3. Diminished RA signaling in the head/forebrain and heart/aortic arches in *LgDel*, but not $Tbx1^{+/-}$ E10.5 embryos. Embryos in (**A**) and (**D**) carry DR5-RARE:βgal RA reporter transgene. (A) βgal labeling in the forebrain (fb) and eye (e; top panels) and the heart/aortic arches (H/AA; dotted lines) in E10.5 WT and *LgDel* embryos. βgal labeling is diminished in the forebrain/head (compare arrowheads, top right) and aortic arches (compare arrowheads, bottom right) of *LgDel* versus WT (9 WT and 6 *LgDel* embryos analyzed). (**B**) Diminished βgal activity in dissected *LgDel* head and heart based upon soluble βgal assays (ONPG). (**C**) *Rar*β expression declines significantly in the forebrain/head in *LgDel* embryos, while both *Raldh2* and *Rar*β expression decline in the heart (solid purple bars). (**D**) No visible differences in cranial or cardiac βgal labeling in $Tbx1^{+/-}$ versus WT embryos. (**E**) βgal activity (ONPG assay) is statistically equivalent in $Tbx1^{+/-}$ and WT littermates (**F**) Expression levels of *Raldh2* and *Rar*β in the head and heart are statistically indistinguishable in $Tbx1^{+/-}$ and WT littermates.

enzymes and receptors parallel these changes (Fig. 3C); *Raldh2* declines significantly in the heart (37%; $n = 7$ *LgDel*, 7 WT; $P \leq 0.04$) and *Rar*β declines significantly in both the head/forebrain and heart (32 and 56%, respectively; $n = 7$ *LgDel*, 7 WT; $P \leq 0.05$). In contrast, in $Tbx1^{+/-}$ embryos, DR5-RARE: βgal activity does not change significantly at either site ($n = 6$ $Tbx1^{+/-}$; 4 WT; Fig. 3D and E). There are no significant changes in the expression levels of *Raldh2* and *Rarβ* in the head/forebrain of $Tbx1^{+/-}$ embryos; however, *Raldh2* declines significantly in the heart (22%, $n = 7$ $Tbx1^{+/-}$, 9 WT; $P \leq 0.003$), in parallel with that in the *LgDel*.

Together, these results establish modest but statistically significant changes as well as local variation of Shh and RA signaling at key 22q11DS phenotypic sites—the forebrain/head and heart in *LgDel*, but not $Tbx1^{+/-}$, embryos. In one case—Shh signaling in the heart—local changes are distinct from those detected in whole embryos (Fig. 1). In contrast, changes of RA signaling and related gene expression in the forebrain/head and heart parallel those measured in the whole embryo.

Shh, RA, Fgf and Bmp signaling influence 22q11 gene expression

Morphogenetic signaling is interactive and homeostatic—signals influence and are modulated by multiple target genes—perhaps to adjust for individual genetic and environmental variation (36,37) including subtle changes in signaling like those we found in *LgDel* embryos. Given the coincident expression of multiple 22q11 genes and morphogenetic signals, it is possible that Shh, RA, Fgfs or Bmps regulate expression of 22q11 genes beyond *Tbx1* (16,17). Thus, we asked if morphogenetic signals regulate 22q11 gene expression during early embryogenesis.

We did an initial comparison of mRNA levels of 22 22q11 genes selectively expressed at 22q11DS phenotypic sites (11) in whole E10.5 embryos carrying constitutive loss- and gain-of-function mutations for morphogenetic signals, or after acute exposure to function blocking agents (a total of 11 genetic or pharmacological manipulations for which we measured expression of 22 22q11 genes plus several controls; $n = 3$ for each mutation or manipulation; Supplementary Material, Fig. S3). This initial analysis identified a subset of genes for each signaling pathway that are consistently and substantially altered by loss or gain of function. From this subset, we selected a small group of 22q11 genes for *in situ* hybridization (ISH) combined with further qPCR analysis to determine whether local patterns of 22q11 gene expression change in response to pharmacologically increased or decreased morphogenetic signaling in WT embryos. For each of four 22q11 genes (Fig. 4), we saw local expression level changes at 22q11DS phenotypic sites (ISH performed on sets of WT treated and untreated embryos in the same vials; $n \geq 4$ WT and treated embryos for each gene) whose direction and magnitude is consistent with qPCR measurements. Expression patterns of these genes were not dramatically expanded or contracted and there were no novel or ectopic expression domains. For some genes, however, expression level changes were not uniform at all 22q11DS phenotypic sites—for example, there is increased *Ranbp1* labeling in the frontonasal process and limb, but not branchial arches or heart following cyclopamine exposure (Fig. 4, top). Evaluation following FgfR inhibition is complicated by altered growth at 22q11DS phenotypic sites (Fig. 4, middle). Together, these results show that some regulation of 22q11 genes by Shh, RA, Fgf and Bmp is possible. This regulation, however, likely reflects local modulation of expression levels—or overall growth—at 22q11DS phenotypic sites rather than substantial changes in patterning of the embryo.

22q11 gene dosage and Shh signaling interact during morphogenesis

Our data suggest that interactions between 22q11 gene dosage and local signals influence morphogenesis at 22q11DS phenotypic sites. Environmental or genetic changes, beyond 22q11 deletion but acting on shared targets, could lead to enhanced, diminished or novel phenotypes. Alternately, additional disruption of 22q11 gene expression by dis-regulated signaling might yield loss of function, or dosage rescue of one or more of 22q11 genes with parallel key 22q11DS phenotypic

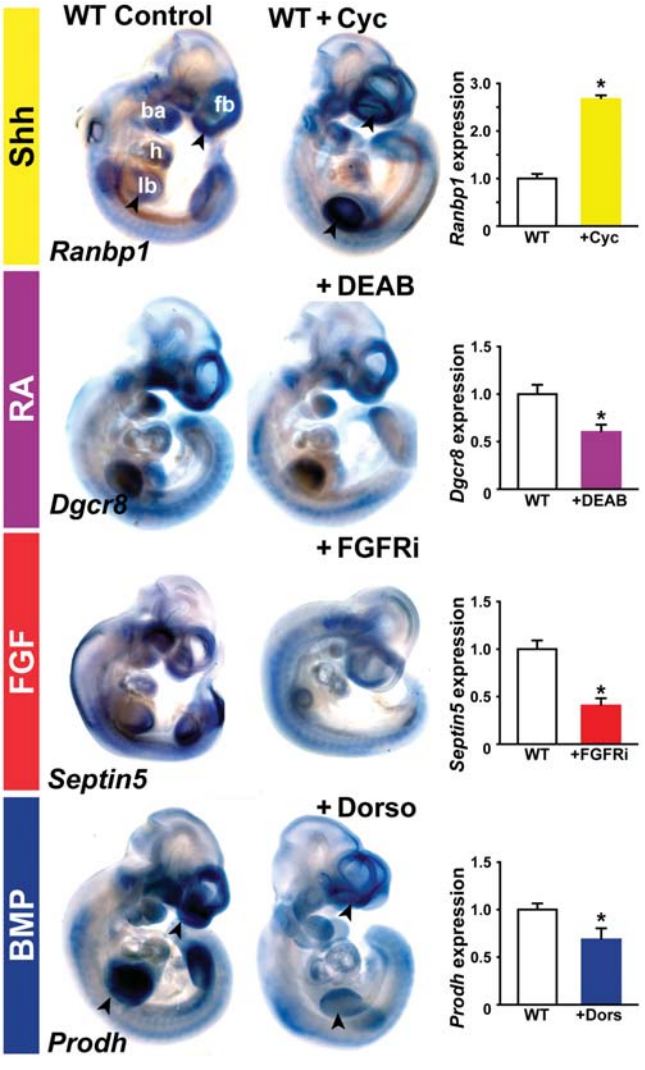

Figure 4. Morphogenetic signals regulate levels of 22q11 gene expression. Representative E10.5 whole embryo *in situ* hybridization (ISH) shows expression patterns and intensity for four 22q11 genes in WT embryos (left) and WT embryos treated pharmacologically to diminish Shh (cyclopamine), RA (DEAB), Fgf (FgfRi) or Bmp (dorsomorphin) signaling. For each gene WT control and WT treated embryos were hybridized and reacted for labeling in the same vials to insure absolutely identical conditions. Sites of mesenchymal/epithelial (M/E) interaction and 22q11DS phenotypes are indicated in the WT control embryo, top left: fb, forebrain; ba, branchial arches; h, heart; lb, limb bud. Black arrowheads indicate instances when expression levels change at some M/E 22q11DS phenotypic sites but not others. At right, mRNA levels in whole WT embryos treated pharmacologically with cyclopamine, DEAB, FgfRi or dorsomorphin have been measured using qPCR for each gene whose expression is localized using ISH. Asterisks indicate statistically significant differences.

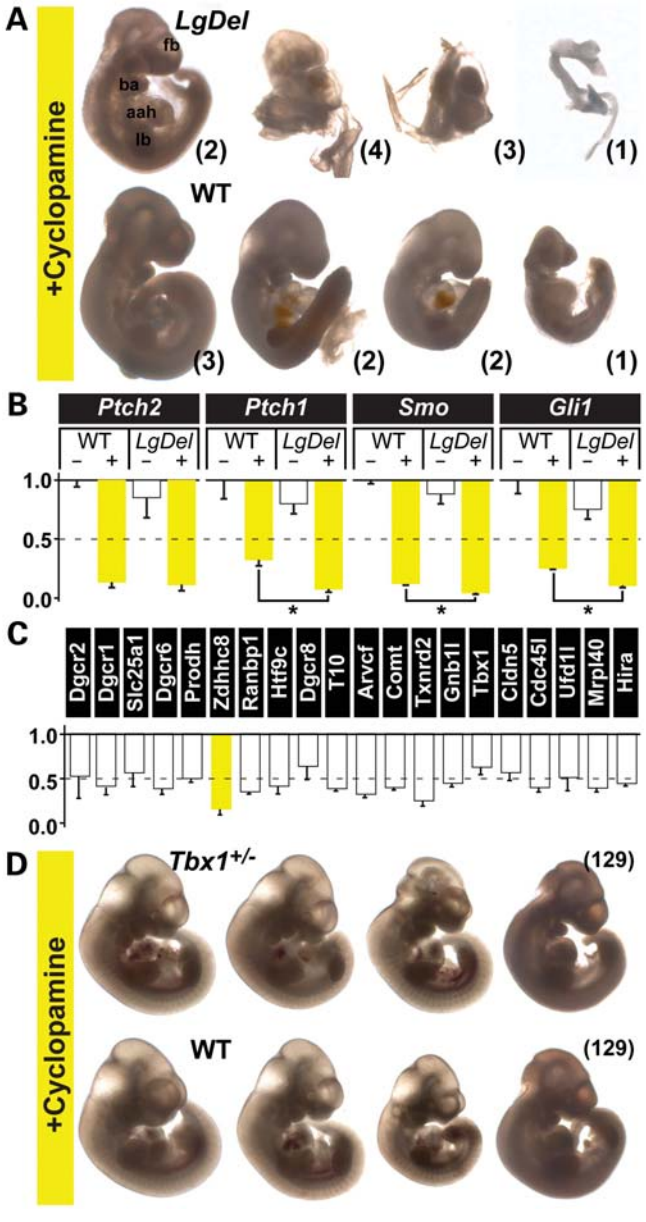

Figure 5. Response of WT, *LgDel* and $Tbx1^{+/-}$ embryos to diminished Shh signaling due to 48 h cyclopamine exposure. (**A**) Consequences of cyclopamine-mediated decline of Shh signaling in *LgDel* versus WT littermates. *LgDel* embryos have far more severe and frequent morphogenetic anomalies at sites of M/E interaction (fb, ba, aah, lb). Numbers of embryos with similar severity of disrupted development are shown in brackets next to each example. (**B**) Transcriptional responses of four Shh-related signaling genes whose expression is modulated by altered Shh signaling (significant differences indicated with brackets and asterisks). (**C**) In *LgDel* embryos, cyclopamine does not significantly diminish expression of most 22q11 genes, with the exception of *Zdhhc8*, beyond the 50% decrement seen in *LgDel* alone. (**D**) Consequences of cyclopamine-mediated decline in Shh signaling for $Tbx1^{+/-}$ versus WT littermate embryos. Although there is some variation in size, there are no noticeable changes in differentiation of non-axial structures.

changes. Thus, we altered Shh signaling levels in *LgDel* and WT littermates between E8.5 and E10.5 with sub-teratogenic doses of cyclopamine (38) or *Shh* and *Gli3* mutations, and assessed consequences for morphogenesis and gene expression.

Cyclopamine-exposed *LgDel* embryos are far more compromised than WT littermates (Fig. 5A; $n = 9$ *LgDel*, 8 WT, two litters). Most cyclopamine-treated *LgDel* embryos (77%) fail to develop limb buds, aortic or branchial arches, olfactory placodes, eyes and forebrains, whereas cyclopamine-treated WT embryos, even though some are dysmorphic, develop these structures. In parallel, there is an equivalent decline (80%) of *Shh*-regulated *Ptch2* in *LgDel* and WT embryos (Fig. 5B; $n = 3$ *LgDel*, 3 *LgDel* + cyclo., 3 WT, 3 WT + cyclo.).

Additional Shh signaling genes, however, are significantly more diminished in cyclopamine-exposed *LgDel* embryos, including *Ptch1* (93% *LgDel*; 68% WT; $P \leq 0.01$), *Smo* (96% *LgDel*; 88% WT; $P \leq 0.02$) and *Gli1* (90% *LgDel*; 75% WT; $P \leq 0.003$). In contrast, 22q11 gene expression—except for *Zdhhc8* (for which homozygous deletion does not result in obvious morphogenetic change; 39)—is not diminished beyond 50% in cyclopamine treated *LgDel* embryos (Fig. 5C; $n = 3$ *LgDel* + cyclo., 3 *LgDel*; $P \leq 0.0002$ for *Zdhhc8*), including 22q11 genes that change in response to cyclopamine in WT embryos (Fig. 4 and Supplementary Material, Fig. S3). Finally, cyclopamine-treated $Tbx1^{+/-}$ embryos do not differ morphologically from WT littermates ($n = 7$ $Tbx1^{+/-}$; $n = 9$ WT embryos from two litters; Fig. 5D). Apparently, diminished 22q11 gene dosage—beyond *Tbx1*—sensitizes mid-gestation embryos to deleterious effects of substantially reduced *Shh* activity. Cyclopamine-induced dysmorphology in WT embryos from *Tbx1* litters is less noticeable than in WT embryos from *LgDel* litters, independent of genetic background (Fig. 5D). This may reflect systemic maternal responses due to the resorption of cyclopamine-exposed *LgDel* embryos that also compromise WT littermates (40,41).

We confirmed this apparent interaction between *Shh* and 22q11 dosage genetically using $Shh^{+/-}$ (42), $Gli3^{+/Xtj}$ and $Gli3^{Xtj/Xtj}$ (43) mutants in combination with *LgDel*. For rigorous assessment of phenotypic modulation, we quantified a specific 22q11DS morphogenetic phenotype seen clearly in *LgDel* embryos—4th pharyngeal arch artery hypoplasia (PAA4; Fig. 6A). In $Shh^{+/-}$ embryos, expression of *Smo*, *Ptch1* and *Ptch2*, all *Shh*-regulated (44), are not altered ($P \geq 0.4$, $n = 5$), even though *Shh* declines by 40% ($P \leq 0.007$, $n = 6$ $Shh^{+/-}$; 4 WT), and *Gli3* increases by 16% ($P \leq 0.03$; Fig. 6B). We saw no gross phenotypic changes in *LgDel*:$Shh^{+/-}$ embryos (data not shown). Forty-four percent (4/9) of $Shh^{+/-}$:*LgDel* embryos have a hypoplastic or absent PAA4, statistically indistinguishable from the 57% PAA4 frequency in *LgDel* littermates ($P \leq 0.2$; Table 1). We selected *Gli3* as a likely *Shh* gain-of-function mutation based upon its established role in *Shh*-mediated repression (45). Surprisingly, *Shh* itself as well as two positive regulators of Shh signaling are reduced rather than increased—the anticipated consequence of release of repression—in $Gli3^{+/Xtj}$ and $Gli3^{Xtj/Xtj}$ embryos (Fig. 6C). In $Gli3^{+/Xtj}$ embryos, *Gli1* was reduced to 61% of WT ($P \leq 0.03$, $n = 10$ $Gli3^{+/Xtj}$; 8 WT). In $Gli3^{Xtj/Xtj}$ embryos, *Gli1*, *Smo* and *Shh* were reduced to 29, 53 and 60% of WT ($P \leq 0.02$ $n = 5$ $Gli3^{Xtj/Xtj}$; 8 WT), respectively. Together these data suggest that *Gli3* mutation results in diminished, rather than enhanced Shh signaling. One hundred percent of $Gli3^{Xtj/+}$:*LgDel* ($n = 8/8$) and $Gli3^{Xtj/Xtj}$:*LgDel* ($n = 6/6$) embryos have significant PAA4 disruptions seen at significantly lower frequency or not at all in WT, *LgDel* or *Gli3* mutants (Fig. 6D; $Gli3^{+/Xtj}$:*LgDel* $P \leq 0.005$; $Gli3^{Xtj/Xt}$:*LgDel* $P \leq 0.01$; Table 1). Thus, in *LgDel* embryos, diminished *Shh* in $Shh^{+/-}$ mutants is insufficient to modify 22q11DS phenotypes, whereas decreased Shh signaling in cyclopamine treated *LgDel* as well as $Gli3^{Xtj}$:*LgDel* embryos reaches a threshold for phenotypic change not seen in WT littermates, single mutants or $Tbx1^{+/-}$ embryos.

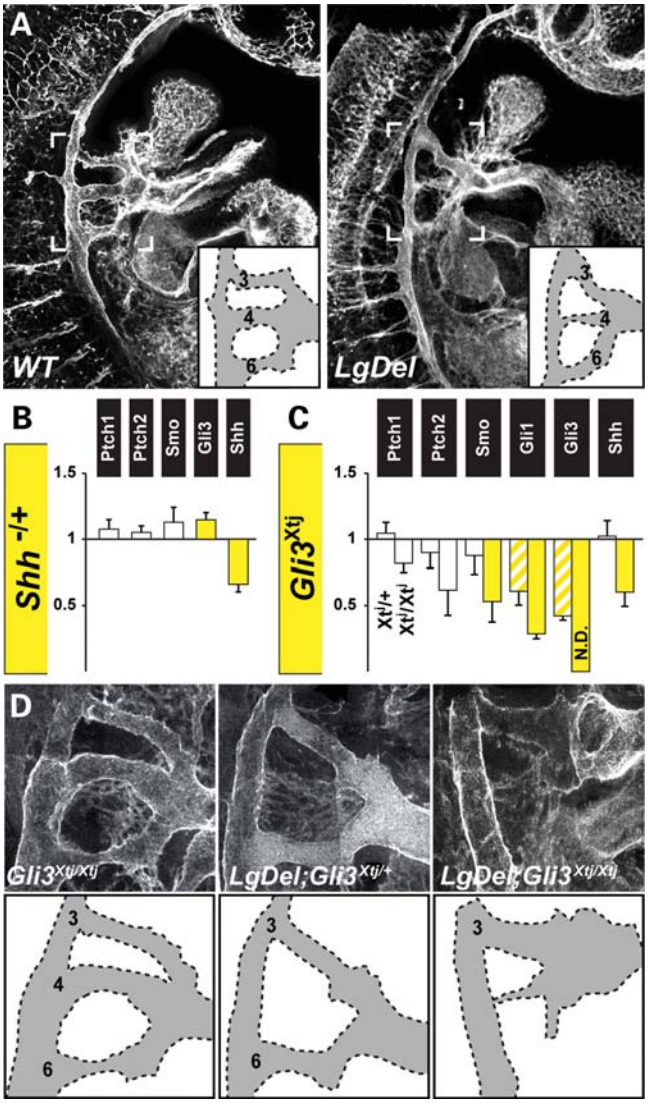

Figure 6. Genetic alteration of Shh signaling selectively modifies gene expression and cardiac phenotypes in *LgDel* embryos. (**A**) Lower magnification Z-stack confocal images showing the heart and pharyngeal arch arteries (PAA) in E10.5 WT and *LgDel* embryos stained for the cell-adhesion molecule PECAM/CD31, and imaged whole. The primary *LgDel* phenotype is a hypoplastic PAA4 (compare at double arrowheads). (**B**) Changes in expression levels of Shh-regulated genes in E10.5 $Shh^{+/-}$ embryos. Solid yellow bars indicate significant changes. (**C**) Changes in a broader range of Shh-regulated genes in E10.5 $Gli3^{+/Xtj}$ (left hand bar in each pair) and $Gli3^{Xtj/Xtj}$ (right hand bar in each pair) embryos. Hatched ($Gli3^{+/Xtj}$) and solid ($Gli3^{Xtj/Xtj}$) yellow bars indicate significant changes. (**D**) Higher magnification confocal images of PECAM labeled PAAs in $Gli3^{Xtj/Xtj}$, *LgDel*:$Gli3^{+/Xtj}$ (middle) and *LgDel:*$Gli3^{Xtj/Xtj}$ (right). The PAAs in the $Gli3^{Xtj/Xtj}$ are comparable to WT. Compound mutants have increasingly severe and more frequent PAA4 and PAA6 hypoplasia not seen in *LgDel* or $Gli3^{+/Xtj}$ or $Gli3^{Xtj/Xtj}$ mutant embryos (Table 1). The tracings in the lower panels highlight primary phenotypic changes.

22q11 gene dosage and RA signaling interact during morphogenesis

If a proposed 'phenocopy' of 22q11DS due to RA loss-of-function (13) reflects linear relationships between RA signaling and 22q11 gene dosage, enhanced signaling should

Table 1. The consequences of genetically altered Shh signaling via the *Shh* or the *Gli3*^{Xtj} mutation on pharyngeal arch artery 4 (PAA4) morphogenesis in *LgDel* embryos, based on frequency of hypoplastic or absent PAA4

	4th arch phenotype			
	Total	Normal	Hypoplastic	Absent
WT	33	33	0	0
Lgdel	33	15	18	0
Shh$^{-/+}$	9	9	0	0
LgDel;*Shh*$^{-/+}$	9	5	3	1
Gli3$^{XtJ/+}$	9	9	0	0
Gli3$^{XtJ/+}$;*Lgdel*	8	0	4	4
Gli3$^{XtJ/XtJ}$	5	5	0	0
Gli3$^{XtJ/XtJ}$;*LgDel*	4	0	1	3

Single or compound genotypes are listed at left, and frequency of PAA4 dysmorphology is given in middle and right hand columns.

result in rescue, and decreased signaling should have little influence on 22q11DS phenotypes. This would be consistent with diminished levels of RA signaling we have found in *LgDel* embryos. If, however, the relationship between 22q11 and RA signaling reflects more complex homeostatic interactions with 22q11 gene dosage, either raising or lowering RA signaling could lead to significantly enhanced or novel phenotypes.

Modest, sustained doses of *all trans* RA delivered via maternal circulation between E8.5 and E10.5, similar to those reported to rescue RA-related mutant phenotypes (46), substantially increase RA signaling levels. Based on DR5-RARE quantification, 48 h RA exposure increases RA signaling in the head/forebrain by 73% for WT ($n = 4$; $P \leq 0.02$) and 50% for *LgDel* embryos ($n = 4$; $P \leq 0.02$). In the heart, there is a divergent response: *LgDel* embryos have a significant increase (38%, $n = 4$, $P \leq 0.03$); WT embryos do not (18%, $n = 4$ $P \geq 0.14$). Thus, diminished 22q11 gene dosage differentially modulates cranial versus cardiac RA signaling. These changes are accompanied by disruption of cranial and cardiovascular morphogenesis in RA-exposed *LgDel* embryos not seen in RA-exposed WT littermates or untreated *LgDel* embryos (Fig. 7A). RA-treated *LgDel* embryos have significantly increased neural tube closure defects—a phenotype not routinely associated with 22q11DS [but see Nickel and Magenis (47)] 11/15 *LgDel* + RA versus 0/39 WT + RA and 0/33 *LgDel* untreated are exencephalic ($P \leq 0.0001$; Table 2). Cardiac phenotypes are also modified. PAA dysmorphology is substantially enhanced in RA-treated *LgDel* versus WT littermates or untreated *LgDel* embryos (Fig. 7B; Table 3). PAA4 defects reach 100%, and PAA4 is frequently absent (5/8 in *LgDel* + RA; 0/8 *LgDel*; $P \leq 0.01$; Fig. 7B, Table 3). These novel anomalies are not seen at significantly higher levels in RA-treated *Tbx1*$^{+/-}$ embryos (Tables 2 and 3). Thus, diminished 22q11 gene dosage beyond *Tbx1* interacts with elevated RA signaling in the developing brain and heart to yield substantially altered phenotypes.

We next asked whether increased RA signaling in the *LgDel* differentially modifies RA-signaling gene expression. Expression of several genes that are either unchanged (*Raldh1*) or diminished in *LgDel* embryos (*Raldh2*, *Rar*α,

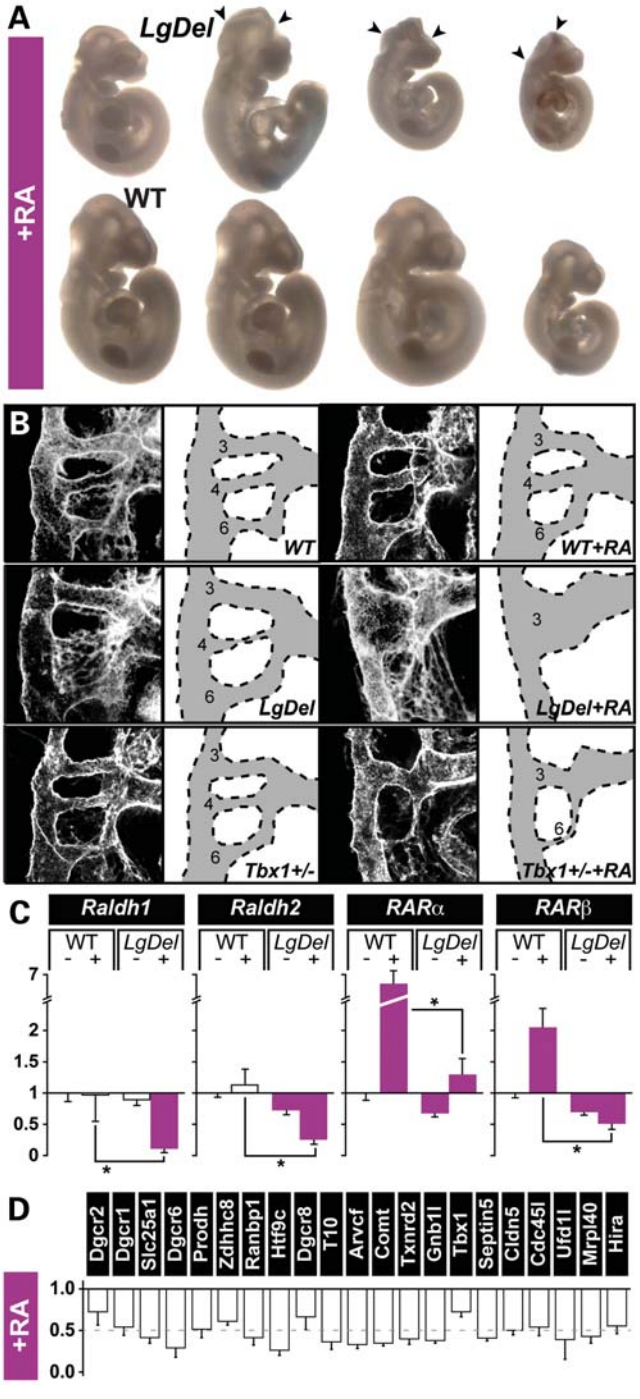

Figure 7. Diminished dosage of 22q11 genes sensitizes embryos to subteratogenic RA exposure. (**A**) RA-exposed *LgDel* (top half) are substantially more dysmorphic and smaller in size than WT littermates (bottom half; 15 *LgDel* and 19 WT littermate embryos from four litters). (**B**) Confocal images, and accompanying tracings, of PECAM-labeled PAAs in untreated WT, *LgDel* and *Tbx1* embryos show the normal pattern (WT and WT + RA) and varying degrees of dysmorphology in *LgDel* and *Tbx1*$^{+/-}$ as well as *LgDel* and *Tbx1*$^{+/-}$ treated with RA. (**C**) Distinct expression changes in RA signaling-related genes in *LgDel* embryos. Brackets and asterisks indicate significant differences in expression levels between the four groups (WT – and + RA; *LgDel* – and + RA). (**D**) Increased RA between E8 and E10 does not significantly alter 22q11 gene expression beyond 50% in E10.5 *LgDel* embryos.

Table 2. The consequences of pharmacological or genetic alteration of RA signaling for neural tube closure in *LgDel* embryos, based on scoring for exencephaly at E10.5

	Total	Normal	Exencephalic
WT	39	39	0
WT + RA	19	19	0
LgDel	33	33	0
LgDel + RA	15	4	11
Tbx1$^{+/-}$	10	10	0
Tbx1$^{+/-}$ + RA	7	7	0
Raldh2$^{+/-}$	14	14	0
LgDel;*Raldh2*$^{+/-}$	11	7	4
Tbx1$^{+/-}$;*Raldh2*$^{+/-}$	5	5	0

Genotypes and RA treatment groups are identified at left, and the frequency of exencephaly is recorded at right.

Table 3. The consequences of pharmacological or genetic alteration of RA signaling for PAA4 morphogenesis in *LgDel* embryos

	4th arch phenotype			
	Total	Normal	Hypoplastic	Absent
WT	33	33	0	0
WT + RA	11	8	3	0
LgDel	33	15	18	0
LgDel + RA	8	0	3	5
Tbx1$^{+/-}$	10	6	4	0
Tbx1$^{+/-}$ + RA	7	3	2	2
Raldh2 $^{+/-}$	14	13	1	0
LD;*Raldh2*$^{+/-}$	8	2	2	4
Tbx1;*Raldh2*$^{+/-}$	9	3	6	0

Genotypes and RA treatment groups are identified at left, and the frequency of PAA dysmorphology, scored as hypoplastic or absent, is listed in the middle and right hand columns.

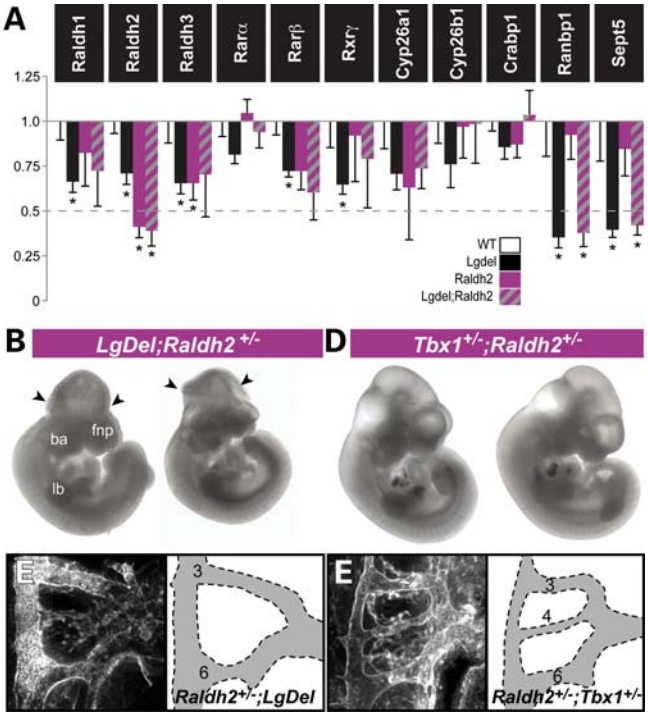

Figure 8. Genetic alteration of RA signaling selectively modifies cranial and cardiac phenotypes in *LgDel* embryos. (**A**) RA regulated RA signaling genes are diminished in *LgDel* and *LgDel*:*Raldh2*$^{+/-}$ embryos. Asterisks indicate RA-regulated or 22q11 genes whose expression is significantly altered from WT levels in *Raldh2*$^{+/-}$, *LgDel* and *Raldh2*$^{+/-}$:*LgDel* compound embryos. There is no apparent interaction between the two genotypes for further change in RA-regulated genes. (**B**) Morphogenetic phenotypes, including smaller limb buds (lb) and branchial arches (ba), diminished frontonasal processes (fnp), and exencephaly (arrowheads) are seen in compound *LgDel*:*Raldh2*$^{+/-}$ embryos. (**C**) Confocal image and accompanying cartoon of PAAs in *LgDel*:*Raldh2*$^{+/-}$ embryos show PAA4 absence. (**D**) *Tbx1*$^{+/-}$:*Raldh2*$^{+/-}$ compound mutant embryos have no observable gross phenotypes. (**E**) PAA morphology in *Tbx1*$^{+/-}$:*Raldh2*$^{+/-}$ compound mutants.

*Rar*β; Fig. 1) is further decreased by RA exposure (Fig. 7C; $n = 3$ *LgDel* + RA, 3 *LgDel*, 3 WT + RA, 3 WT; $P \leq 0.04$ *Raldh1*, 0.02 *Raldh2*, 0.005 *Rar*α, 0.03 *Rar*β). Indeed, for two RA-regulated retinoid receptors, *Rar*α and *Rar*β, RA has divergent effects in WT and *LgDel* embryos. In contrast, despite some indication that RA influences 22q11 gene expression (Fig. 4 and Supplementary Material, Fig. S3), there is no significant change for any 22q11 genes in RA-treated *LgDel* embryos beyond the 50% diminished expression seen in untreated *LgDel* embryos (Fig. 7D; $n = 3$ *LgDel* + RA, 3 *Lgdel*; see also Supplementary Material, Fig. S3). Therefore, diminished 22q11 gene dosage differentially alters the transcriptional response to elevated RA signaling without modifying 22q11 gene expression.

Finally, we asked whether *LgDel* embryos are also sensitized to a genetic mutation that modestly lowers RA signaling. E10.5 mouse embryos carrying a heterozygous *Raldh2* mutation (48) have 20% diminished RA signaling levels based on quantitative assessment using the DR5-RARE reporter ($P \leq 0.002$, $n = 4$), without obvious dysmorphology. This change has consequences for RA-regulated gene expression in *Raldh2*$^{+/-}$ as well as *Raldh2*$^{+/-}$:*LgDel* embryos (Fig. 8A). In each of the three genotypes, levels are often significantly lower than WT (asterisks); however, there are no significant differences between *Raldh2*$^{+/-}$ and *Raldh2*$^{+/-}$:*LgDel* embryos. Moreover, selected 22q11 genes (apparently RA-regulated; Fig. 4 and Supplementary Material, Fig. S3) do not decline beyond the 50% *LgDel* values in either additional genotype (Fig. 8A, right). To determine if a potentially compound decrease of RA signaling due to heterozygous *Raldh2* mutation and diminished 22q11 dosage results in novel or enhanced 22q11DS related phenotypes, we assessed neural tube closure and PAA4 development in *Raldh2*$^{+/-}$:*LgDel* compound mutants. Thirty-six percent (4/11) of *Raldh2*$^{+/-}$:*LgDel* mutants exhibit exencephaly not observed in *LgDel*, *Raldh2*$^{+/-}$ or WT embryos ($P \leq 0.02$; Fig. 8B and Table 3). One hundred percent of *Raldh2*$^{+/-}$;*LgDel* embryos have PAA4 dysmorphogenesis, whereas littermate *LgDel* embryos have the expected 57% frequency (Table 3; $P = 0.02$). In compound mutants, PAA4 phenotypes (Fig. 8C) include hypoplasia (4/8; 50%) as well as absence (4/8; 50%). These phenotypes are seen at significantly higher frequencies in *Raldh2*$^{+/-}$;*LgDel* embryos versus single or compound *Raldh2*$^{+/-}$:*Tbx1*$^{+/-}$ mutant embryos ($P \leq 0.01$; Table 3; Fig. 8D and E). The frequency of PAA4

hypoplasia (66%) is statistically indistinguishable in *Tbx1*$^{+/-}$ and *Raldh2*$^{+/-}$:*Tbx1*$^{+/-}$ embryos ($n = 6/9$ *Raldh2*$^{+/-}$:*Tbx1*$^{+/-}$; 4/10 *Tbx1*$^{+/-}$; $P = 0.2$). Thus, diminished 22q11 gene dosage sensitizes *LgDel*, but not *Tbx1*$^{+/-}$ embryos to both elevated and diminished RA signaling, resulting in novel or more severe 22q11DS-related cranial and cardiac phenotypes.

DISCUSSION

When 22q11 gene expression is diminished, signaling via Shh and RA is altered in the developing brain and heart. These changes may directly influence embryonic phenotypes associated with 22q11DS; however, they also enhance sensitivity of cranial and cardiac development to additional Shh or RA signaling variation. Alteration of RA and Shh signaling that is minimally disruptive in WT or *Tbx1* mutant embryos causes more frequent, severe or novel phenotypes in *LgDel* embryos. Apparently, full dosage of multiple 22q11 genes establishes an optimal adaptive range for Shh and RA signaling in the developing head and heart. 22q11 deletion constricts this range and diminishes embryonic tolerance to signaling variability. Thus, the mutable frequency and severity of 22q11DS phenotypes—particularly forebrain and heart anomalies—likely reflects, in part, consequences of otherwise relatively benign environmental exposure or genetic variation that alters morphogenetic signaling beyond adaptive levels that are constricted by diminished 22q11 gene dosage.

Quantitative alterations of morphogenetic signaling in 22q11DS

Four essential morphogenetic signaling pathways—activated by Shh, RA, Fgfs and Bmps—have been associated with 22q11DS pathogenesis for the last two decades (12,13,15,16,18,23,33,49,50). Some pathways have been implicated based upon apparent phenotypic similarities in mutant mice and 22q11DS (49,50), while altered expression patterns of selected target genes, especially in *Tbx1* mutant mice, indicate contributions by others (16–19,33,51). We found that diminished 22q11 gene dosage, beyond *Tbx1*, regulates expression levels of Shh, RA and Bmp—and to a lesser extent Fgf—signaling genes. These pathways in turn regulate 22q11 gene expression levels. This apparently reciprocal regulation, however, is limited. Altered Shh or RA signaling in *LgDel* embryos does not further reduce 22q11 gene expression (with one exception) beyond 50%. Finally, the magnitude or direction of changes in signaling and signal-dependent 22q11 gene expression varies at 22q11DS phenotypic sites including the brain and heart. Such distinctions provide a new framework for considering complex and variable 22q11DS phenotypes. Local quantitative changes in signaling and 22q11 gene dosage during mid-gestation likely modulate morphogenetic interactions between mesenchymal (M) and epithelial (E) tissues at these sites. Phenotypes may vary due to altered M/E signaling that idiosyncratically further modifies morphogenetic signaling activity in the context of diminished 22q11 dosage.

22q11 gene dosage and Shh signaling interact during morphogenesis

We found that diminished 22q11 gene dosage—exclusive of *Tbx1*—disrupts Shh signaling levels in the heart, and sensitizes embryos to deleterious effects of altered Shh signaling. In the heart, epithelial Shh may maintain a minimal level of 22q11 gene expression in the mesenchyme and establish feedback that further regulates epithelial Shh signaling centers (52). Diminished dosage of 22q11 genes may disrupt this relationship leading to the local increase in cardiac *Shh* and Shh signaling we found. This may reflect altered inductive capacity of neural crest derived cardiac mesenchyme (12,14,46,53) with 22q11-related epithelial disruption of *Shh* leading to additional mesenchymal changes. Shh is required for cardiac neural crest survival (54) and maintenance of heart field progenitor proliferation (55). Thus, the local gain in *Shh* message and Shh signaling in the heart (or stability in the forebrain despite embryo-wide diminished *Shh* expression in the *LgDel*) may defray or modify some consequences of decreased 22q11 gene dosage (16,56). Indeed, compensatory changes in Shh signaling may be an M/E-mediated local response to embryo-wide *Shh* decline in the context of diminished 22q11 gene dosage.

When Shh signaling is disrupted briefly but substantially—based upon decline in levels of *Ptch1, Ptch2* and *Smo*—following cyclopamine exposure, non-axial morphogenesis fails in *LgDel* but not WT or *Tbx1*$^{+/-}$ embryos. Therefore, diminished 22q11 gene dosage beyond *Tbx1* sensitizes some essential aspect of *Shh*-mediated M/E-dependent morphogenesis at 22q11DS phenotypic sites. Cell proliferation may be a key target, since both Shh signaling and several 22q11 genes enhance proliferation (9,57). The combined consequences of cyclopamine-altered Shh signaling and diminished 22q11 dosage, especially in the mesenchyme where *Shh* is mitogenic (58) and 22q11 gene expression is enhanced (11) may overwhelm morphogenesis. Shh signaling is apparently diminished by *Gli3* mutation based on declines in the *Gli1* transcriptional activator (*Gli3*$^{+/Xtj}$ and *Gli3*$^{Xtj/Xtj}$) as well as *Smo* and *Shh* itself (*Gli3*$^{Xtj/Xtj}$). Partial or complete loss of *Gli3* activator or repressor function may disrupt a precarious equilibrium of already modified Shh signaling leading to more severe phenotypes. Apparently, 22q11 deletion compromises the normal balance of Shh signaling in the heart, and thus alters the threshold for cardiac morphogenetic modulation by additional genetic or environmental changes in Shh signaling.

RA signaling pathways are disrupted by 22q11 deletion

Appropriate 22q11 gene dosage—again exclusive of *Tbx1*—maintains the integrity of RA signaling in *LgDel* embryos. Decreased expression of two out of three major RA synthetic enzymes, *Raldh2* and *Raldh3,* essential for brain and heart development (59) as well as two RA-regulated receptors, *Rar*β (60) and *Rar*α, in *LgDel* embryos, all expressed primarily in the mesenchyme at 22q11DS phenotypic sites (11,52,61), may modify mesenchymal RA production (52,62) thus disrupting RA signaling in adjacent epithelia in *LgDel* embryos. Such changes might compromise proliferation or differentiation in progenitors that rely upon RA signaling in the

brain (63) and cardiac outflow tract (64). Thus, deletion of multiple 22q11 genes critical for RA signaling, especially 22q11 genes expressed selectively or exclusively in cranial and pharyngeal arch mesenchyme (11 and unpublished data), may interfere with the ability of cranial or cardiac tissues to generate, transmit or metabolize RA resulting in locally decreased RA signaling and brain and heart dysmorphogenesis.

We found that a sub-teratogenic increase in RA signaling (~50%) or a modest decline (20%) due to heterozygous mutation of *Raldh2* has surprisingly similar morphogenetic consequences in *LgDel* but not WT, *Raldh2*$^{+/-}$ or *Tbx1*$^{+/-}$ embryos. This accords with many observations that demonstrate similar effects of increased or diminished RA signaling on morphogenesis (65). In both *LgDel* + RA and *LgDel*:*Raldh2*$^{+/-}$ embryos, RA-regulated genes have distinct transcriptional responses when 22q11 deletion and altered RA signaling are combined. Nevertheless, in both instances, there is novel occurrence of exencephaly as well as increased frequency and severity of PAA dysmorphogenesis. This consistent outcome, despite divergent RA-mediated transcriptional regulation, demonstrates—contrary to earlier claims based on studies in *Tbx1* mutant embryos (18,33,66)—that singular changes in RA-sensitive genes like *Rar*β, *Rar*α or other RA cofactors, are unlikely to explain specific cranial or cardiovascular phenotypes as 22q11DS phenocopies.

Morphogenetic disruptions in *LgDel*:*Raldh2*$^{+/-}$ embryos cannot be explained by modulation of RA signaling levels or related RA signaling gene expression alone. Indeed, expression of key RA signaling genes in the *LgDel*:*Raldh2*$^{+/-}$ compound mutant embryos is essentially indistinguishable from that in *Raldh2*$^{+/-}$ embryos. It is likely that transcriptional disruptions in the *LgDel*:*Raldh2*$^{+/-}$ engage multiple targets including additional signaling pathways and downstream effectors. Diminished 22q11 gene expression alters key Shh and BMP signaling genes in parallel with changes in RA signaling. These pathways, whose activity is known to be modified in the forebrain or heart of Raldh2 mutant mice (67,68), and many others, might be more significantly compromised by simultaneous 22q11 gene deletion and heterozygous *Raldh2* mutation than either alone. A broader analysis of transcriptome changes in single and compound mutants may identify such synergistic, quantitative disruptions of homeostatic regulation of networks beyond those directly engaged in RA signaling. Thus, additive disruptions, beginning with a single signaling pathway and expanding to include multiple gene networks, may contribute to phenotypic variation seen in 22q11DS.

22q11 gene dosage establishes a dynamic range for morphogenetic interactions

Our data show that full 22q11 gene dosage—exclusive of *Tbx1*—maintains an adaptive range for morphogenetic signaling in the heart and brain (Fig. 9). Accordingly, when 22q11 gene dosage is diminished in 22q11DS, or elevated, as in instances of 22q11 duplication (69,70), M/E interactions that drive heart and brain morphogenesis no longer accommodate modest to substantial changes in Shh and RA signaling that otherwise do not result in phenotypes. A broad range of altered Shh signaling, from 20 to 80% based on measurement

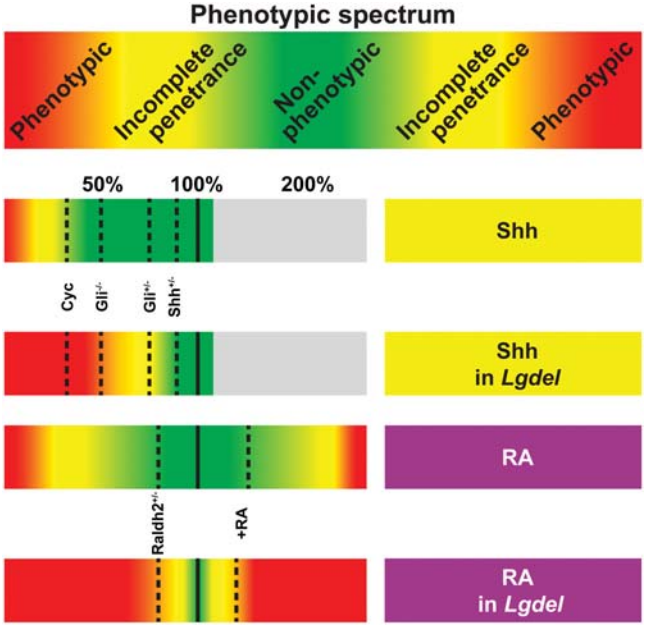

Figure 9. Diminished dosage of 22q11 genes constricts an adaptive range for optimal morphogenetic signaling. First row: Optimal adaptive range for morphogenetic signaling. In this model, signaling via Shh, RA (or, potentially, other morphogenetic signals that act at M/E sites) might fall a considerable amount below or above an optimal level (100%) before phenotypic consequences are seen. Second row: Adaptive range for Shh signaling buffers against phenotypic changes when Shh signaling is reduced by as much as 86% in WT embryos. Third row: Diminished 22q11 gene expression constricts the adaptive range of Shh signaling and modifies levels of aberrant signaling that can be tolerated without phenotypic change. Fourth row: The adaptive range for RA signaling in WT extends from ~80 to 173% WT signaling levels, based upon our data. Fifth row: The adaptive range for RA signaling is constricted when 22q11 gene expression is diminished, and novel or more severe phenotypes are seen.

of *Ptch1, Ptch2, Gli1* or *Smo* (Fig. 9) is tolerated fairly well by WT, *Shh*$^{+/-}$, *Gli3*$^{+/-}$ or *Gli3*$^{-/-}$ but not *LgDel* embryos. Similarly, a 50% increase or 20% decline defines a range of RA signaling that can be accommodated in the head and heart of WT and *Tbx1*$^{+/-}$, but not *LgDel* embryos (Fig. 9). Thus, otherwise benign changes of Shh or RA signaling may explain a substantial amount of 22q11DS phenotypic variation (2). Such changes may arise from fairly common environmental and genetic disruptions (71,72), and these aberrations when combined with diminished 22q11 gene dosage likely modulate 22q11DS phenotypic severity. Diminished dosage of *Tbx1* alone does not constrict the adaptive range for Shh and RA signaling; instead, diminished dosage of additional 22q11 genes—the fundamental change in 22q11DS patients—is necessary. Accordingly, deletion of 22q11 genes beyond *Tbx1* likely interacts with otherwise benign alterations in morphogenetic signaling to enhance clinically significant phenotypes in individuals with 22q11DS.

MATERIALS AND METHODS

Mice

The University of North Carolina at Chapel Hill (UNC-CH) Division of Laboratory Animal Medicine or The George

Washington (GW) University Animal Research Facility maintained colonies of WT CD-1, *Shh*$^{+/-}$, *Gli3*$^{+/-}$, *Fgf8*$^{neo/+}$, *Raldh2*$^{+/-}$, *Nog*$^{+/-}$, *Tbx1*$^{+/-}$, DR5-RARE:βgal and *Ptch2*:βgal (Deltagen) mice. All mutant lines were maintained on a C57BL6/J6 background. We also used *Tbx1* mutants on an S129 background for cyclopamine exposure experiments. The *LgDel* mutation [heterozygous deletion on mmchr.16 from *Idd* to *Hira* (30)] was transmitted paternally. Timed-pregnant females (vaginal plug day = E0.5) were sacrificed by rapid cervical dislocation and embryos were dissected and collected for expression, signaling or phenotypic analysis. All procedures were reviewed and approved by the Institutional Animal Care and Use Committee (IACUC) at UNC-CH or GW.

Quantitative PCR (qPCR)

E10.5 embryos (or dissected embryonic regions as described) were harvested, dissected and homogenized in TRIzol (Invitrogen). Total RNA was isolated, and cDNA synthesized and qPCR performed as described previously (10). Primers for qPCR are listed in Supplementary Material, Table S1. Expression of each transcript is displayed as the fraction of the expression in the WT and untreated cohort.

Statistical analysis

Mean expression values between genotypes or treatments were compared using Student's unpaired *t*-test. Fisher's exact tests, used to compare phenotypic outcomes in groups with distinct genotypes, were conducted using MS Excel software.

Immunohistochemistry and ISH

Embryos were fixed overnight, and ISH and imaging was performed as described previously (9). For whole mount immuno-staining, embryos were dehydrated in methanol, stored at -80°C and freeze-thawed (5×). Specimens were rehydrated (PBS) and then incubated overnight at 4°C in 5% DMSO, 0.2% Triton X-100 and 5% normal goat serum in PBS. Following primary antibody incubation overnight at 4°C (Rat anti-CD31/PECAM; BD-Pharmingen), specimens were rinsed and labeled with Alexa-Fluor 488 or 546 conjugated anti-rat secondary antibodies overnight (4°C). Finally, embryos were rinsed and dehydrated in MeOH, cleared with 2:1 benzyl alcohol:benzyl benzoate and imaged on a Zeiss LSM 510 confocal microscope. 2D projections of Z-Stacks were created using Zeiss LSM image processing software.

β-galactosidase staining and enzymatic activity quantification

Embryos were harvested and dissected in PBS and either fixed in 0.1% glutaraldyhyde for whole mount staining or lysed in 2 × ONPG (ortho-Nitrophenyl-βgalactoside) lysis buffer (Promega) for soluble βgal assays as described previously (62). βgal activity was detected as a function of ONPG enzymatic hydrolysis analyzed at 420 nm on an ELX808 ultra microplate reader (Bio-Tek Instruments).

Pharmacological treatments

To evaluate regulation of 22q11 genes in WT embryos, pregnant WT dams (CD-1 strain) were injected with 10 mg/kg RA (Sigma), 100 mg/kg DEAB (Sigma), 80 mg/kg cyclopamine (LC Laboratories), 50 mg/kg PD173074 (Sigma) or 10 mg/kg dorsomorphin (Sigma) at E9.5 and embryos harvested 24 h later. To evaluate consequences of disrupted *Shh* or RA signaling for morphogenesis, pregnant *LgDel* dams were injected with RA (10 mg/kg on E8.5 and 20 mg/kg on E9.5) or cyclopamine (80 mg/kg) twice (E8.5 and E9.5) over 48 h period before harvesting at E10.5.

SUPPLEMENTARY MATERIAL

Supplementary Material is available at *HMG* online.

ACKNOWLEDGEMENTS

We thank Yongqin Wu and Megumi Aita for performing the *in situ* hybridization and Amanda Peters, Matthew Fralish and Thomas Harrigan for technical assistance.

Conflict of Interest statement. There have been no influences that might bias the work reported in the results, figures, and tables, or modify any interpretations, implications or opinions stated in the Results and Discussion.

FUNDING

This work was supported by an American Heart Association (grant 0815067E to D.G.), National Institutes of Health (grants NICHD042182 and NIMH64065 to A.-S.L.) as well as NINDS NS031768 to the University of North Carolina Neuroscience Center Expression Profiling and *In Situ* Hybridization core facilities, and S10RR025565 from the National Center for Research Resources for GWU Center for Microscopy Imaging and Analysis.

REFERENCES

1. Shaikh, T.H., Kurahashi, H., Saitta, S.C., O'Hare, A.M., Hu, P., Roe, B.A., Driscoll, D.A., McDonald-McGinn, D.M., Zackai, E.H., Budarf, M.L. *et al.* (2000) Chromosome 22-specific low copy repeats and the 22q11.2 deletion syndrome: genomic organization and deletion endpoint analysis. *Hum. Mol. Genet.*, **9**, 489–501.
2. Ryan, A.K., Goodship, J.A., Wilson, D.I., Philip, N., Levy, A., Seidel, H., Schuffenhauer, S., Oechsler, H., Belohradsky, B., Prieur, M. *et al.* (1997) Spectrum of clinical features associated with interstitial chromosome 22q11 deletions: a European collaborative study. *J. Med. Genet.*, **34**, 798–804.
3. Shprintzen, R.J., Goldberg, R.B., Lewin, M.L., Sidoti, E.J., Berkman, M.D., Argamaso, R.V. and Young, D. (1978) A new syndrome involving cleft palate, cardiac anomalies, typical facies, and learning disabilities: velo-cardio-facial syndrome. *Cleft Palate J.*, **15**, 56–62.
4. Chaoui, R., Korner, H., Bommer, C. and Kalache, K.D. (2002) Fetal thymus and the 22q11.2 deletion. *Prenat. Diagn.*, **22**, 839–840.
5. Lindsay, E.A., Morris, M.A., Gos, A., Nestadt, G., Wolyniec, P.S., Lasseter, V.K., Shprintzen, R., Antonarakis, S.E., Baldini, A. and Pulver, A.E. (1995) Schizophrenia and chromosomal deletions within 22q11.2. *Am. J. Hum. Genet.*, **56**, 1502–1503.
6. Amati, F., Conti, E., Novelli, A., Bengala, M., Diglio, M.C., Marino, B., Giannotti, A., Gabrielli, O., Novelli, G. and Dallapiccola, B. (1999)

Atypical deletions suggest five 22q11.2 critical regions related to the DiGeorge/velo-cardio-facial syndrome. *Eur. J. Hum. Genet.*, **7**, 903–909.
7. Fernandez, L., Nevado, J., Santos, F., Heine-Suner, D., Martinez-Glez, V., Garcia-Minaur, S., Palomo, R., Delicado, A., Pajares, I.L., Palomares, M. *et al.* (2009) A deletion and a duplication in distal 22q11.2 deletion syndrome region. Clinical implications and review. *BMC Med. Genet.*, **10**, 48.
8. LaMantia, A.S. (1999) Forebrain induction, retinoic acid, and vulnerability to schizophrenia: insights from molecular and genetic analysis in developing mice. *Biol. Psychiatry*, **46**, 19–30.
9. Meechan, D.W., Tucker, E.S., Maynard, T.M. and LaMantia, A.S. (2009) Diminished dosage of 22q11 genes disrupts neurogenesis and cortical development in a mouse model of 22q11 deletion/DiGeorge syndrome. *Proc. Natl Acad. Sci. USA*, **106**, 16434–16445.
10. Meechan, D.W., Maynard, T.M., Wu, Y., Gopalakrishna, D., Lieberman, J.A. and LaMantia, A.S. (2006) Gene dosage in the developing and adult brain in a mouse model of 22q11 deletion syndrome. *Mol. Cell. Neurosci.*, **33**, 412–428.
11. Maynard, T.M., Haskell, G.T., Peters, A.Z., Sikich, L., Lieberman, J.A. and LaMantia, A.S. (2003) A comprehensive analysis of 22q11 gene expression in the developing and adult brain. *Proc. Natl Acad. Sci. USA*, **100**, 14433–14438.
12. Frank, D.U., Fotheringham, L.K., Brewer, J.A., Muglia, L.J., Tristani-Firouzi, M., Capecchi, M.R. and Moon, A.M. (2002) An Fgf8 mouse mutant phenocopies human 22q11 deletion syndrome. *Development*, **129**, 4591–4603.
13. Vermot, J., Niederreither, K., Garnier, J.M., Chambon, P. and Dolle, P. (2003) Decreased embryonic retinoic acid synthesis results in a DiGeorge syndrome phenotype in newborn mice. *Proc. Natl Acad. Sci. USA*, **100**, 1763–1768.
14. Washington Smoak, I., Byrd, N.A., Abu-Issa, R., Goddeeris, M.M., Anderson, R., Morris, J., Yamamura, K., Klingensmith, J. and Meyers, E.N. (2005) Sonic hedgehog is required for cardiac outflow tract and neural crest cell development. *Dev. Biol.*, **283**, 357–372.
15. Bachiller, D., Klingensmith, J., Shneyder, N., Tran, U., Anderson, R., Rossant, J. and De Robertis, E.M. (2003) The role of chordin/Bmp signals in mammalian pharyngeal development and DiGeorge syndrome. *Development*, **130**, 3567–3578.
16. Garg, V., Yamagishi, C., Hu, T., Kathiriya, I.S., Yamagishi, H. and Srivastava, D. (2001) Tbx1, a DiGeorge syndrome candidate gene, is regulated by sonic hedgehog during pharyngeal arch development. *Dev. Biol.*, **235**, 62–73.
17. Zhang, L., Zhong, T., Wang, Y., Jiang, Q., Song, H. and Gui, Y. (2006) TBX1, a DiGeorge syndrome candidate gene, is inhibited by retinoic acid. *Int. J. Dev. Biol.*, **50**, 55–61.
18. Guris, D.L., Duester, G., Papaioannou, V.E. and Imamoto, A. (2006) Dose-dependent interaction of Tbx1 and Crkl and locally aberrant RA signaling in a model of del22q11 syndrome. *Dev. Cell*, **10**, 81–92.
19. Arnold, J.S., Werling, U., Braunstein, E.M., Liao, J., Nowotschin, S., Edelmann, W., Hebert, J.M. and Morrow, B.E. (2006) Inactivation of Tbx1 in the pharyngeal endoderm results in 22q11DS malformations. *Development*, **133**, 977–987.
20. Braunstein, E.M., Monks, D.C., Aggarwal, V.S., Arnold, J.S. and Morrow, B.E. (2009) Tbx1 and Brn4 regulate retinoic acid metabolic genes during cochlear morphogenesis. *BMC Dev. Biol.*, **9**, 31.
21. Guo, T., McDonald-McGinn, D., Blonska, A., Shanske, A., Bassett, A.S., Chow, E., Bowser, M., Sheridan, M., Beemer, F., Devriendt, K. *et al.* (2011) Genotype and cardiovascular phenotype correlations with TBX1 in 1,022 velo-cardio-facial/DiGeorge/22q11.2 deletion syndrome patients. *Hum. Mutat.*, **32**, 1278–1289.
22. Randall, V., McCue, K., Roberts, C., Kyriakopoulou, V., Beddow, S., Barrett, A.N., Vitelli, F., Prescott, K., Shaw-Smith, C., Devriendt, K. *et al.* (2009) Great vessel development requires biallelic expression of Chd7 and Tbx1 in pharyngeal ectoderm in mice. *J. Clin. Invest.*, **119**, 3301–3310.
23. Vitelli, F., Morishima, M., Taddei, I., Lindsay, E.A. and Baldini, A. (2002) Tbx1 mutation causes multiple cardiovascular defects and disrupts neural crest and cranial nerve migratory pathways. *Hum. Mol. Genet.*, **11**, 915–922.
24. Rauch, R., Hofbeck, M., Zweier, C., Koch, A., Zink, S., Trautmann, U., Hoyer, J., Kaulitz, R., Singer, H. and Rauch, A. (2010) Comprehensive genotype-phenotype analysis in 230 patients with tetralogy of Fallot. *J. Med. Genet.*, **47**, 321–331.
25. Yagi, H., Furutani, Y., Hamada, H., Sasaki, T., Asakawa, S., Minoshima, S., Ichida, F., Joo, K., Kimura, M., Imamura, S. *et al.* (2003) Role of TBX1 in human del22q11.2 syndrome. *Lancet*, **362**, 1366–1373.
26. Jerome, L.A. and Papaioannou, V.E. (2001) DiGeorge syndrome phenotype in mice mutant for the T-box gene, Tbx1. *Nat. Genet.*, **27**, 286–291.
27. Funke, B.H., Lencz, T., Finn, C.T., DeRosse, P., Poznik, G.D., Plocik, A.M., Kane, J., Rogus, J., Malhotra, A.K. and Kucherlapati, R. (2007) Analysis of TBX1 variation in patients with psychotic and affective disorders. *Mol. Med.*, **13**, 407–414.
28. Paylor, R., Glaser, B., Mupo, A., Ataliotis, P., Spencer, C., Sobotka, A., Sparks, C., Choi, C.H., Oghalai, J., Curran, S. *et al.* (2006) Tbx1 haploinsufficiency is linked to behavioral disorders in mice and humans: implications for 22q11 deletion syndrome. *Proc. Natl Acad. Sci. USA*, **103**, 7729–7734.
29. Torres-Juan, L., Rosell, J., Morla, M., Vidal-Pou, C., Garcia-Algas, F., de la Fuente, M.A., Juan, M., Tubau, A., Bachiller, D., Bernues, M. *et al.* (2007) Mutations in TBX1 genocopy the 22q11.2 deletion and duplication syndromes: a new susceptibility factor for mental retardation. *Eur. J. Hum. Genet.*, **15**, 658–663.
30. Merscher, S., Funke, B., Epstein, J.A., Heyer, J., Puech, A., Lu, M.M., Xavier, R.J., Demay, M.B., Russell, R.G., Factor, S. *et al.* (2001) TBX1 is responsible for cardiovascular defects in velo-cardio-facial/DiGeorge syndrome. *Cell*, **104**, 619–629.
31. Liao, J., Kochilas, L., Nowotschin, S., Arnold, J.S., Aggarwal, V.S., Epstein, J.A., Brown, M.C., Adams, J. and Morrow, B.E. (2004) Full spectrum of malformations in velo-cardio-facial syndrome/DiGeorge syndrome mouse models by altering Tbx1 dosage. *Hum. Mol. Genet.*, **13**, 1577–1585.
32. Lania, G., Zhang, Z., Huynh, T., Caprio, C., Moon, A.M., Vitelli, F. and Baldini, A. (2009) Early thyroid development requires a Tbx1-Fgf8 pathway. *Dev. Biol.*, **328**, 109–117.
33. Roberts, C., Ivins, S., Cook, A.C., Baldini, A. and Scambler, P.J. (2006) Cyp26 genes a1, b1 and c1 are down-regulated in Tbx1 null mice and inhibition of Cyp26 enzyme function produces a phenocopy of DiGeorge Syndrome in the chick. *Hum. Mol. Genet.*, **15**, 3394–3410.
34. Passman, J.N., Dong, X.R., Wu, S.P., Maguire, C.T., Hogan, K.A., Bautch, V.L. and Majesky, M.W. (2008) A sonic hedgehog signaling domain in the arterial adventitia supports resident Sca1+ smooth muscle progenitor cells. *Proc. Natl Acad. Sci. USA*, **105**, 9349–9354.
35. Balkan, W., Colbert, M., Bock, C. and Linney, E. (1992) Transgenic indicator mice for studying activated retinoic acid receptors during development. *Proc. Natl Acad. Sci. USA*, **89**, 3347–3351.
36. Miletich, I., Yu, W.Y., Zhang, R., Yang, K., Caixeta de Andrade, S., Pereira, S.F., Ohazama, A., Mock, O.B., Buchner, G., Sealby, J. *et al.* (2011) Developmental stalling and organ-autonomous regulation of morphogenesis. *Proc. Natl Acad. Sci. USA*, **108**, 19270–19275.
37. Salazar-Ciudad, I. and Jernvall, J. (2010) A computational model of teeth and the developmental origins of morphological variation. *Nature*, **464**, 583–586.
38. Lipinski, R.J., Hutson, P.R., Hannam, P.W., Nydza, R.J., Washington, I.M., Moore, R.W., Girdaukas, G.G., Peterson, R.E. and Bushman, W. (2008) Dose- and route-dependent teratogenicity, toxicity, and pharmacokinetic profiles of the hedgehog signaling antagonist cyclopamine in the mouse. *Toxicol. Sci.*, **104**, 189–197.
39. Mukai, J., Liu, H., Burt, R.A., Swor, D.E., Lai, W.S., Karayiorgou, M. and Gogos, J.A. (2004) Evidence that the gene encoding ZDHHC8 contributes to the risk of schizophrenia. *Nat. Genet.*, **36**, 725–731.
40. Baines, M.G., Duclos, A.J., de Fougerolles, A.R. and Gendron, R.L. (1996) Immunological prevention of spontaneous early embryo resorption is mediated by non-specific immunosimulation. *Am. J. Reprod. Immunol.*, **35**, 34–42.
41. Duclos, A.J., Haddad, E.K. and Baines, M.G. (1995) Presence of activated macrophages in a murine model of early embryo loss. *Am. J. Reprod. Immunol.*, **33**, 354–366.
42. Chiang, C., Litingtung, Y., Lee, E., Young, K.E., Corden, J.L., Westphal, H. and Beachy, P.A. (1996) Cyclopia and defective axial patterning in mice lacking Sonic hedgehog gene function. *Nature*, **383**, 407–413.
43. Schimmang, T., Lemaistre, M., Vortkamp, A. and Ruther, U. (1992) Expression of the zinc finger gene Gli3 is affected in the morphogenetic mouse mutant extra-toes (Xt). *Development*, **116**, 799–804.

44. Katoh, Y. and Katoh, M. (2009) Hedgehog target genes: mechanisms of carcinogenesis induced by aberrant hedgehog signaling activation. *Curr. Mol. Med.*, **9**, 873–886.
45. Blaess, S., Corrales, J.D. and Joyner, A.L. (2006) Sonic hedgehog regulates Gli activator and repressor functions with spatial and temporal precision in the mid/hindbrain region. *Development*, **133**, 1799–1809.
46. Niederreither, K., Vermot, J., Messaddeq, N., Schuhbaur, B., Chambon, P. and Dolle, P. (2001) Embryonic retinoic acid synthesis is essential for heart morphogenesis in the mouse. *Development*, **128**, 1019–1031.
47. Nickel, R.E. and Magenis, R.E. (1996) Neural tube defects and deletions of 22q11. *Am. J. Med. Genet.*, **66**, 25–27.
48. Niederreither, K., Subbarayan, V., Dolle, P. and Chambon, P. (1999) Embryonic retinoic acid synthesis is essential for early mouse post-implantation development. *Nat. Genet.*, **21**, 444–448.
49. Sulik, K.K., Cook, C.S. and Webster, W.S. (1988) Teratogens and craniofacial malformations: relationships to cell death. *Development*, **103** (suppl.), 213–231.
50. Johnston, M.C. and Bronsky, P.T. (1991) Animal models for human craniofacial malformations. *J. Craniofac. Genet. Dev. Biol.*, **11**, 277–291.
51. Roberts, C., Ivins, S.M., James, C.T. and Scambler, P.J. (2005) Retinoic acid down-regulates Tbx1 expression in vivo and in vitro. *Dev. Dyn.*, **232**, 928–938.
52. Bhasin, N., Maynard, T.M., Gallagher, P.A. and LaMantia, A.S. (2003) Mesenchymal/epithelial regulation of retinoic acid signaling in the olfactory placode. *Dev. Biol.*, **261**, 82–98.
53. Bockman, D.E., Redmond, M.E. and Kirby, M.L. (1989) Alteration of early vascular development after ablation of cranial neural crest. *Anat. Rec.*, **225**, 209–217.
54. Goddeeris, M.M., Schwartz, R., Klingensmith, J. and Meyers, E.N. (2007) Independent requirements for Hedgehog signaling by both the anterior heart field and neural crest cells for outflow tract development. *Development*, **134**, 1593–1604.
55. Dyer, L.A. and Kirby, M.L. (2009) Sonic hedgehog maintains proliferation in secondary heart field progenitors and is required for normal arterial pole formation. *Dev. Biol.*, **330**, 305–317.
56. Roberts, C., Sutherland, H.F., Farmer, H., Kimber, W., Halford, S., Carey, A., Brickman, J.M., Wynshaw-Boris, A. and Scambler, P.J. (2002) Targeted mutagenesis of the Hira gene results in gastrulation defects and patterning abnormalities of mesoendodermal derivatives prior to early embryonic lethality. *Mol. Cell. Biol.*, **22**, 2318–2328.
57. Fuccillo, M., Joyner, A.L. and Fishell, G. (2006) Morphogen to mitogen: the multiple roles of hedgehog signalling in vertebrate neural development. *Nat. Rev. Neurosci.*, **7**, 772–783.
58. Mao, J., Kim, B.M., Rajurkar, M., Shivdasani, R.A. and McMahon, A.P. (2010) Hedgehog signaling controls mesenchymal growth in the developing mammalian digestive tract. *Development*, **137**, 1721–1729.
59. Rhinn, M. and Dolle, P. (2012) Retinoic acid signalling during development. *Development*, **139**, 843–858.
60. Lohnes, D., Mark, M., Mendelsohn, C., Dolle, P., Dierich, A., Gorry, P., Gansmuller, A. and Chambon, P. (1994) Function of the retinoic acid receptors (RARs) during development (I). Craniofacial and skeletal abnormalities in RAR double mutants. *Development*, **120**, 2723–2748.
61. Vaessen, M.J., Kootwijk, E., Mummery, C., Hilkens, J., Bootsma, D. and van Kessel, A.G. (1989) Preferential expression of cellular retinoic acid binding protein in a subpopulation of neural cells in the developing mouse embryo. *Differentiation*, **40**, 99–105.
62. LaMantia, A.S., Colbert, M.C. and Linney, E. (1993) Retinoic acid induction and regional differentiation prefigure olfactory pathway formation in the mammalian forebrain. *Neuron*, **10**, 1035–1048.
63. Sakai, Y., Meno, C., Fujii, H., Nishino, J., Shiratori, H., Saijoh, Y., Rossant, J. and Hamada, H. (2001) The retinoic acid-inactivating enzyme CYP26 is essential for establishing an uneven distribution of retinoic acid along the anterio-posterior axis within the mouse embryo. *Genes. Dev.*, **15**, 213–225.
64. Li, P., Pashmforoush, M. and Sucov, H.M. (2010) Retinoic acid regulates differentiation of the secondary heart field and TGFbeta-mediated outflow tract septation. *Dev. Cell*, **18**, 480–485.
65. Soprano, D.R. and Soprano, K.J. (1995) Retinoids as teratogens. *Annu. Rev. Nutr.*, **15**, 111–132.
66. Caterino, M., Ruoppolo, M., Fulcoli, G., Huynth, T., Orru, S., Baldini, A. and Salvatore, F. (2009) Transcription factor TBX1 overexpression induces downregulation of proteins involved in retinoic acid metabolism: a comparative proteomic analysis. *J. Proteome. Res.*, **8**, 1515–1526.
67. Ribes, V., Wang, Z., Dolle, P. and Niederreither, K. (2006) Retinaldehyde dehydrogenase 2 (RALDH2)-mediated retinoic acid synthesis regulates early mouse embryonic forebrain development by controlling FGF and sonic hedgehog signaling. *Development*, **133**, 351–361.
68. Ryckebusch, L., Wang, Z., Bertrand, N., Lin, S.C., Chi, X., Schwartz, R., Zaffran, S. and Niederreither, K. (2008) Retinoic acid deficiency alters second heart field formation. *Proc. Natl Acad. Sci. USA*, **105**, 2913–2918.
69. Lo-Castro, A., Galasso, C., Cerminara, C., El-Malhany, N., Benedetti, S., Nardone, A.M. and Curatolo, P. (2009) Association of syndromic mental retardation and autism with 22q11.2 duplication. *Neuropediatrics*, **40**, 137–140.
70. Portnoi, M.F. (2009) Microduplication 22q11.2: a new chromosomal syndrome. *Eur. J. Med. Genet.*, **52**, 88–93.
71. Cooper, M.K., Wassif, C.A., Krakowiak, P.A., Taipale, J., Gong, R., Kelley, R.I., Porter, F.D. and Beachy, P.A. (2003) A defective response to Hedgehog signaling in disorders of cholesterol biosynthesis. *Nat. Genet.*, **33**, 508–513.
72. Lammer, E.J., Chen, D.T., Hoar, R.M., Agnish, N.D., Benke, P.J., Braun, J.T., Curry, C.J., Fernhoff, P.M., Grix, A.W. Jr., Lott, I.T. *et al.* (1985) Retinoic acid embryopathy. *N. Engl. J. Med.*, **313**, 837–841.